Contract No.:

This manuscript has been authored by Battelle Savannah River Alliance (BSRA), LLC under Contract No. 89303321CEM000080 with the U.S. Department of Energy (DOE) Office of Environmental Management (EM).

Disclaimer:

The United States Government retains and the publisher, by accepting this article for publication, acknowledges that the United States Government retains a non-exclusive, paid-up, irrevocable, worldwide license to publish or reproduce the published form of this work, or allow others to do so, for United States Government purposes.

Growth interface study of CdTeSe crystals grown by the THM technique

Utpal N Roy[1†], Giuseppe S Camarda[2], Yonggang Cui[2] and Ralph B. James[1]

[1]Savannah River National Laboratory, Aiken, SC 29808, USA.
[2]Brookhaven National Laboratory, Upton, New York 11973, USA.

Abstract:

The Traveling Heater Method (THM) is a widely accepted technique to grow high-quality detector grade CdTe and CdZnTe ingots, especially for X-ray and gamma-ray detector applications. Unlike melt-growth techniques, the growth interface for ingots produced by the THM technique consists of two different compounds, viz. the solidified region (just below the interface) consists of the compound to be grown (e.g., CdZnTe for CdZnTe growth), while the molten zone just above the growth interface consists of Te-rich CdZnTe. Thus, optimization of the growth parameters is critical to obtain a clean growth interface with the required shape and presence of minimal Te-rich inclusions. In this study CdTeSe ingots were grown employing the THM technique to investigate the growth interface. Both macroscopic and microscopic behavior of the interface were studied. The study revealed that a microscopically smooth growth interface can be achieved by optimizing the growth parameters, which is essential for obtaining high-quality, inclusion-free ingots.

Keywords: A2. Crystal growth; A1**.** Growth interface; A2. Traveling heater method; B2. II-VI semiconductor; A1. Radiation detector; B2. Cadmium telluride selenide

[†]Corresponding author: Utpal.Roy@srnl.doe.gov.

1. Introduction

CdTe based II-VI compounds, especially CdZnTe (CZT) with 10 atomic % of Zn, have been the prime candidates for room temperature detector applications for the X- and gamma-ray region for more than three decades [1-6]. On the other hand, another potential candidate (CdTeSe) from the same family was mostly ignored over this time period. Fiederle et al. [7] reported an enhancement of the charge collection efficiency and better homogeneity of the electrical properties compared to CdTe and $Cd_{0.9}Zn_{0.1}Te$ by a partial replacement of tellurium with selenium (CdTeSe). The concentrations of deep levels were also reported to be reduced in CdTeSe (CTS) [7], with the mobility-lifetime product [$(\mu\tau)_e$] of 4.2×10^{-4} cm^2/V for electrons. Later, a much higher $(\mu\tau)_e$ value of 6.55×10^{-2} cm^2/V was reported for CTS with high compositional homogeneity [8]. Afterward, THM-grown CTS was reported to have a $(\mu\tau)_e$ value of 4×10^{-3} cm^2 /V with the resistivity of 5×10^8 Ω-cm, and the material was found to be free from any sub-grain boundary network (dislocation walls) and with reduced concentrations of Te inclusions and very high compositional homogeneity [9-11]. The material was also reported to have reduced deep-level trap densities as compared to CZT [12,13]. Although many observed material properties of CTS were found to be superior to CZT, detectors for high energy gammas could not be achieved due to the material's relatively low electrical resistivity ($<10^{10}$ ohm-cm) and associated thermal noise. For high energy gamma radiation, the required resistivity of the material should be at least $1\text{-}3\times10^{10}$ ohm-cm. The band gap of CdTeSe is known to decrease below the band gap of CdTe with increasing selenium due to lattice disorder [14]. Thus, it is necessary to increase the band gap of the material to achieve a resistivity of $>10^{10}$ ohm-cm. To increase the band gap, cadmium was partially replaced by 10 atomic % Zn in the CdTeSe compound. The resulting compound $Cd_xZn_{1-x}Te_ySe_{1-y}$ (CZTS) fulfills the band-gap requirement, plus high resistivity in the range of $1\text{-}3\times10^{10}$ ohm-cm was attained. The material properties of the new quaternary compound are superior to the presently available CZT material. Presently, the CZT material contains high concentrations of Te inclusions and sub-grain boundary networks. In addition, the grown ingots suffer from compositional inhomogeneity due to the high segregation coefficient of Zn (~1.35) [15-18]. All these defects are known to be performance-limiting defects and severely degrade the detector response. The new selenium-containing quaternary material $Cd_xZn_{1-x}Te_ySe_{1-y}$ is free from sub-grain boundary network, has reduced Te inclusions, and possesses high compositional homogeneity [19-24]. An electrical resistivity in the range of $1\text{-}3\times10^{10}$ ohm-cm could be achieved with $(\mu\tau)_e$ value of $4\text{-}5\times10^{-3}$ cm^2 /V [22,25,26]. The partial replacement of tellurium by selenium also results in a reduction of the density of performance limiting deep traps as compared to CZT [27,28]. Thus, the material quality of CZTS supersedes CZT and is promising for producing a high yield of detector-grade material. The detectors based on CZTS have already demonstrated an ability to outperform CZT-based devices for some medical imaging and homeland security applications [28,29].

It has been demonstrated by several authors that partial replacement of tellurium by selenium offer several advantages compared to CdTe/CZT. The CdTe/CZT detector-grade materials are generally grown by the traveling heater method due to several advantages over melt growth techniques. Hence, the growth interface behavior of selenium containing CdTe-based materials by THM technique demands a systematic study, which has not been reported to date. In this report, we report the first results on the macro- and microscopic behavior at the growth interface of CdTeSe for ingots grown by the THM technique.

2. Experimental

CdTeSe ingots were grown by the THM technique using tellurium as the solvent. The ingots were grown unseeded in conically tipped quartz ampoules with an internal diameter of 22 mm and outer diameter of 25.8 mm. The nominal concentrations of selenium were maintained at 10%, and the material was synthesized using 99.9999% pure CdTe procured from 5N Plus, Inc. and 99.9999% pure CdSe from Azelis Electronics. To avoid the reaction of cadmium with the inner wall of the quartz ampoule, the inner wall of the ampoule was coated with carbon. The ampoules were first cleaned with acetone; next methanol rinsing followed a cleaning by dilute HF. The ampoule was then thoroughly rinsed with freshly prepared deionized water. Carbon coating of the inner wall of the ampoules was performed by pyrolyzing high-purity acetone at 950 °C, followed by baking the coated ampoule at about 1100 °C for an hour. After cooling to room temperature, the coated ampoule was thoroughly cleaned with acetone and dried. The ampoule was then loaded with stoichiometric amounts of CdTe and CdSe to synthesis the ternary compound $CdTe_{0.9}Se_{0.1}$. The ampoule was sealed under a dynamic vacuum of 2×10^{-6} torr. The synthesis was carried out in a three-zone vertical furnace. After placing the ampoule inside the vertical furnace, the temperature of the furnace slowly increased so that the temperature near the tip reaches about 1110 °C and about 1130 °C near the upper part of the ampoule. The temperature was maintained for 72 hours for complete synthesis, and then the temperature of the furnace lowered down to room temperature at a rate of ~ 200 °C/day. The synthesized material and tellurium were then loaded into a freshly prepared carbon-coated quartz ampoule. The tellurium used in the growth experiments was from Alfa Aesar with a purity of 99.9999%. The loaded ampoule was sealed under a dynamic vacuum of $2x10^{-6}$ torr. The loaded ampoule was then placed vertically inside the three-zone furnace. The temperature of the three zones were then slowly increased and set accordingly, so that the temperature near the growth interface was ~850 °C. The growth was carried out at a rate of 3-5 mm/day under a temperature gradient of 10-15 °C/cm. The translation of the ampoule was actuated by a multi-geared DC motor. After the completion of growth, the furnace was slowly cooled to room temperature at a rate of 100 °C/day.

To study the morphology of the growth interface, wafers were cut along the ingot length near the growth interface. Wafers were also cut perpendicular to the growth direction near/below the growth interface for transmission infrared (IR) imaging measurements. All the samples, including the wafer containing the growth interfaces, were lapped with different grit sizes of SiC, followed by polishing successively with different sizes of alumina suspension having diameters of 5 µm, 3 µm, 1 µm, 0.5 µm and 0.05 µm using a felt pad. The mirror-finish polished samples were then used for microscopic analyses both in reflection and IR transmission mode using a Nikon, Eclipse LV 100 Microscope.

3. Results and discussion

The as-grown ingots could be easily removed from the quartz ampoules due to the protective carbon coating at the inner wall of the ampoule. Figure 1 shows a typical $CdTe_{0.9}Se_{0.1}$ ingot with diameter of 22 mm and ~11-cm long, grown by the THM technique. The shiny region on the extreme right of the ingot is the Te-rich CTS zone, and the arrow indicates the CTS/Te-rich growth interface. The optical photograph of the semi-polished wafer, cut along the growth direction of the ingot near the interface, is shown in Figure 2 (a). The dark portion represents grown CdTeSe, while the relatively shiny part is the Te-rich CdTeSe region, and the interface between these two regions is the growth interface. The overall shape of the interface is convex towards the Te-rich solvent, which is preferable for large grain/single crystalline growth. In addition, defects formed at the growth interface generally travel perpendicular to the growth

interface, and for convex growth interfaces the defects tend to move towards the periphery of the grown ingot. A concave

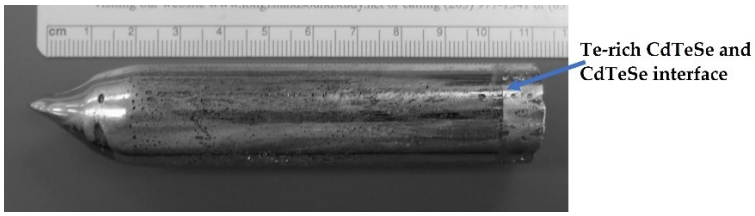

Figure 1. THM-grown 22 mm diameter $CdTe_{0.9}Se_{0.1}$ ingot.

growth interface causes the growth of polycrystalline ingots. Here, the defects travel towards the center of the grown ingot. Thus, the overall macroscopic shape of the growth interface is critical to obtain high-quality ingots. The microscopic irregularities of the growth interface are responsible for the formation of Te inclusions due to trapping of Te-rich CdTeSe in the grown ingot near the growth interface. Thus, optimization of the growth parameters for THM growth is essential to achieve a smooth convex growth interface. Various parameters such as growth temperature, growth rate, temperature gradient near the growth interface and across the molten zone, and height of the molten zone translate to the preferred amount of tellurium used for the molten zone. All these parameters are however interrelated. Optimization of the height of the Te-rich CdSeTe molten zone is the most vital parameter. However, the ideal height does not depend only on the amount of tellurium added to the molten zone. The height of the molten zone for a fixed amount of added tellurium also depends on the growth temperature, temperature gradient, and growth rate. For example, the height of the Te-rich CdSeTe molten zone increases with growth temperature since at higher temperature the Te-rich zone dissolves more amount of feed material thereby increases the zone height. Disruption of the stability of the growth interface mainly arises due to the convection current in the molten zone induced by the temperature gradient and solute concentration gradient. Again, the zone height strongly influences the convection current in the molten zone [30]. The fluid flow becomes stronger for larger zone heights and forms multiple vortex structures, which eventually cause constitutional supercooling near the growth interface, leading to morphological instability at the interface. For a given height of the zone, the constitutional supercooling effect becomes more prominent at higher growth rates [30]. Funaki et al. [31] demonstrated the effect of zone height on the shape of the growth interface for 50-mm diameter CdTe ingots grown by the THM technique. A convex-shaped growth interface was obtained with the optimum zone height, while larger or shorter zone heights produced overall convex shape with some inflection points, which were responsible for the formation of grain boundaries [31]. There are several techniques reported to achieve smooth convex growth interfaces, among them THM growth under a static magnetic field was found to be successful in suppressing the convective flow, resulting in a more uniform concentration and temperature distribution, producing a smooth and stable growth interface [32,33]. The accelerated crucible rotation technique (ACRT) was also reported to be very successful in producing CdZnTe crystals by the THM technique. This technique produced stable convex growth interfaces with microscopically smooth morphology and increased growth rate. Both experimental and theoretical observations agree well for growth conditions to produce better crystals with the desired smooth convex growth interface [34-37]. The ACRT provides better mixing of the liquid zone by imposing forced convection and interrupting buoyancy driven convective flow. Zhou et al. [37] demonstrated a concave to convex to flat growth interface for

53-mm diameter CZT growth without ACRT and with optimized ACRT parameters. The flat growth interface yielded a single crystalline ingot with a small grain near the periphery of the wafer [37]. In the recent past, applying a very low constant rotation of 2.5 RPM (rotations per minute) and 1.25 RPM for 2- and 3-inch diameter CZT ingots by the THM technique was reported to achieve smooth convex growth interfaces, although it was concave for the zero-rotation condition [38]. The very low applied constant rotation was assumed to be sufficient to weaken the natural convection flow resulting in a convex growth interface [38]. Thus, in general reduced natural convection flow is more favorable to attain a convex growth interface. In the present study, we conducted THM growth at a low temperature gradient of 10-15 °C/cm. Figure 2 (b) shows the scanning microscopic image of the same slice taken in the reflection mode. Upon optimization of the growth parameters, especially the content of Te and growth temperature, a smooth convex growth interface was achieved as is evident from Figure 2 (b). As mentioned earlier, the top shiny part of the cross-sectional wafer is the Te-rich CTS zone, and the bottom part is the grown CdTeSe. The growth interface is slightly convex with smooth morphology. The absence of microscopic irregularities at the growth interface suggests a stable growth condition, hence no trapping of Te-rich CTS was observed near the interface. A few cracks are evident as indicated by the arrows in Fig. 2 (b). The occurrence of such cracks near the interface are due to the difference of the thermal expansion coefficient of Te-rich CTS and the grown CTS region. The occurrence of such cracks is common for CdTe or CdZnTe for the same reason. It is to be noted that due to severe cracks near the growth interface, especially for THM grown ingots, investigating the interface under the IR transmission mode is difficult. However, although several cracks are present in our sample, we were able to explore the interface under IR transmission mode, perhaps for the first time for THM-grown CdTe/CZT ingots. Figure 2 (c) shows a scanning microscopic image of the same slice taken in IR transmission mode. As in the reflection mode, IR transmission also suggests a very smooth convex growth interface, without any microscopic irregularity indicating a stable growth interface. However, as indicated by the arrows (Fig. 2 (c)), in the grown CdTeSe region, the presence of Te inclusions is visible, some of which are long bar-shaped inclusions. These large Te inclusions might have formed due to the trapping of Te-rich CTS solution because of localized instability at the growth interface. Figures 3 (a) and 3 (b) illustrate high magnification images of the growth interface in the reflection and transmission mode, respectively. The interface was microscopically smooth all through the interface from one edge to the other, especially in reflection mode, while in transmission mode, a major portion is affected by the cracks. However, between the cracks, the interface was found to be very smooth as observed under the high magnification microscopic analyses. Similar behavior was also observed for a two-inch diameter CZT ingot grown by the THM technique [39]. A microscopically smooth growth interface could be achieved for THM-grown CZT using a low temperature gradient of 10 to 15 °C/cm. Thus, the growth under a low temperature gradient is also found to be effective in achieving a convex growth interface for this selenium-containing compound.

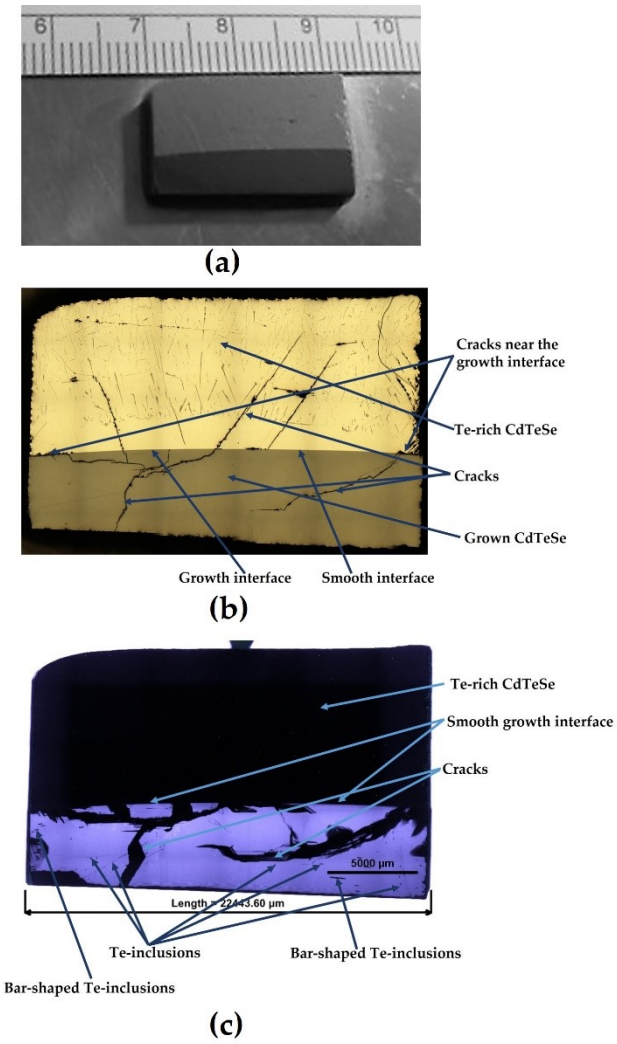

Figure 2. Cross-section of the growth interface. **(a)** Optical photograph of a slice cut parallel to the growth direction showing the growth interface, **(b)** scanning microscopic image of the same slice taken in reflection mode showing a smooth convex growth interface, and **(c)** scanning microscopic image of the same slice taken in the IR transmission mode.

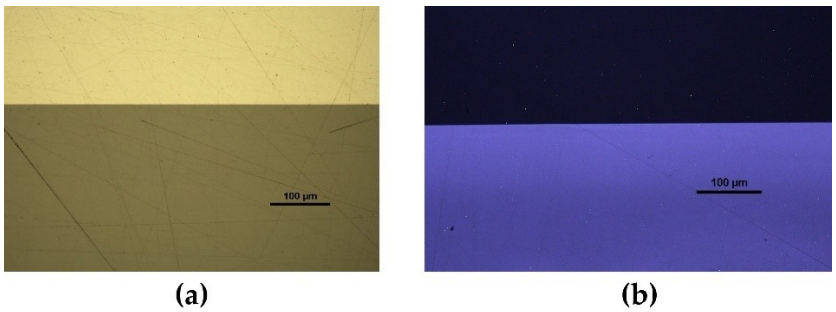

Figure 3. Morphology of the growth interface at high magnification in **(a)** reflection and **(b)** IR transmission mode.

Figure 4 shows an IR transmission microscopic image of two long bar-shaped Te inclusions with a length of ~800 and 400 µm formed possibly due to a localized temperature fluctuation that

perturbed the growth interface and caused trapping of Te-rich CdTeSe. The wafer cut perpendicular to the ingot axis from the position below the growth interface is shown in Figure 5 (a). Although the growth interface shape obtained was convex, which is favorable for producing single crystalline ingots, our wafer contained 2-3 large grains and a few twins. Figure 5 (b) shows the IR transmission scanning microscopic image of the whole wafer of thickness ~ 2 mm. As mentioned, cracks are readily generated near the interface due to the different thermal

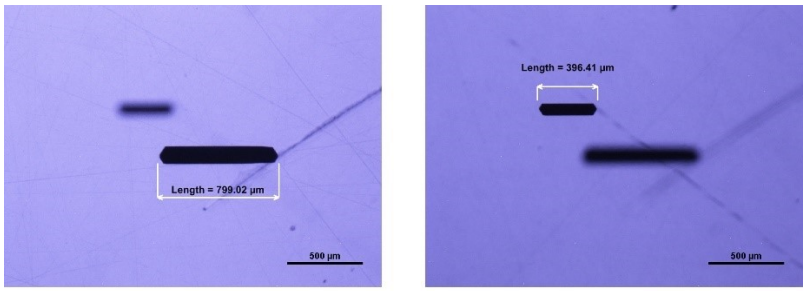

Figure 4. IR transmission microscopic image of two long bar-shaped Te inclusions shown in **(a)** and **(b)**.

expansion coefficient of Te-rich CTS and the grown CTS. Here, the wafer contained a small crack. During lapping process, the crack propagated laterally and along the thickness of the wafer. The crack is visible in the IR transmission image. The grain boundaries are decorated with Te inclusions as indicated in the figure, which is common for the CdTe family of crystals. Large Te inclusions are visible inside the wafer, which were possibly generated due to a localized growth instability at the interface. The appearance of such bar-shaped Te inclusions however was not observed in all the ingots. Figure 6 shows the IR transmission scanning microscopic image of the whole wafer taken from another ingot grown using the same growth parameters. Some Te inclusions were also found to be present at the twin and grain boundaries as indicated in Fig. 5(b), and the magnified microscopic image is shown in Fig. 5c. Other than the large, localized Te inclusions, the wafer is reasonably clean from commonly occurred Te inclusions, typical concentrations, and size distribution of Te-inclusions in as-grown CTS is shown in Fig. 5(d). Fig. 7 (a) shows the microscopic image of the surface in reflection mode, while Figs. 7 (b) and (c) are the IR transmission image from the same spot at different magnifications.

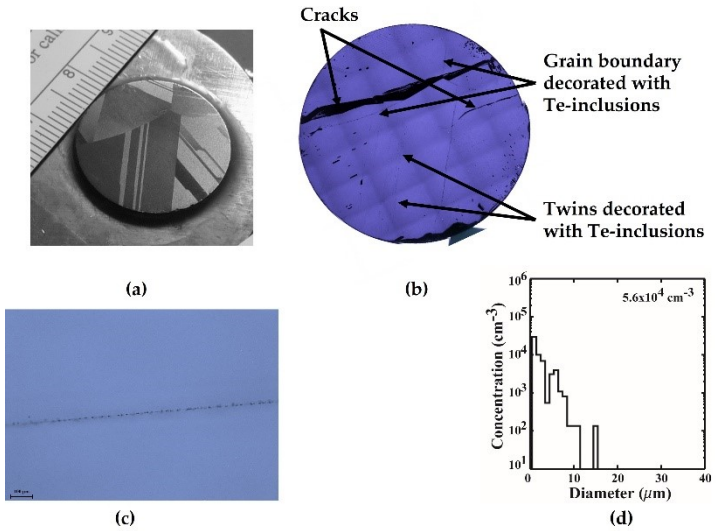

Figure 5. (a) Optical photograph of the semi-polished one-inch diameter wafer cut perpendicular to the ingot axis below the interface, **(b)** IR transmission scanning microscopic image of the whole wafer. (The thickness of the wafer was ~2 mm), **(c)** IR transmission microscopic image of Te-inclusions at twin boundary, and **(d)** size distribution and concentrations of Te inclusions in as-grown CdTeSe.

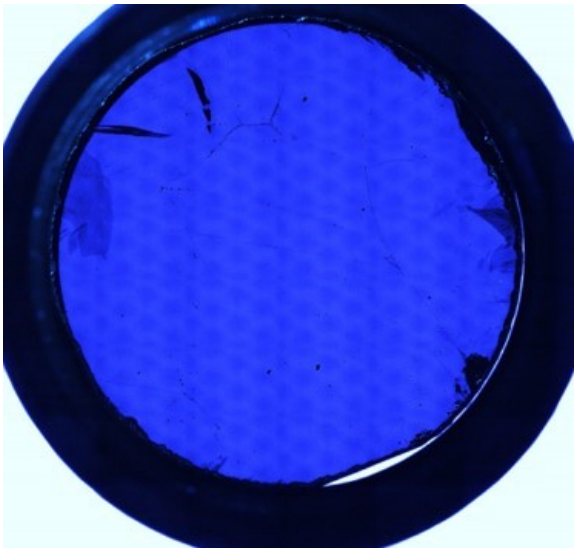

Figure 6. IR transmission scanning microscopic image of the whole wafer of one-inch diameter cut perpendicular from another ingot grown with the same growth parameters.

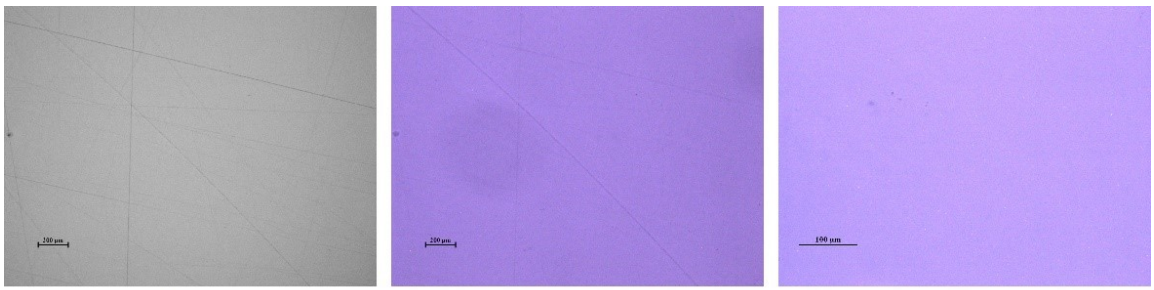

Figure 7. (a) Microscopic image of polished surface in **(a)** reflection and **(b)** IR transmission mode, and **(c)** IR transmission image of the same position at higher magnification.

4. Summary

In this paper we report results on the macro- and microscopic morphology of the growth interface of the selenium-containing material, CdTeSe, for a 10% nominal concentration of selenium. The present investigation showed that after optimization of the growth parameters for THM technique, a microscopically smooth convex growth interface can be achieved for growth under a low-temperature thermal gradient. Thus, growth under a low-temperature gradient can be an alternate path to achieve a smooth convex growth interface as required for low-cost CdTeSe production, as opposed to using an external magnetic field or the more complex ACRT growth technique.

Acknowledgement

This work was partially supported by the U.S. Department of Energy, Office of Defense Nuclear Nonproliferation Research and Development, and the Laboratory Directed Research and Development (LDRD) program within the Savannah River National Laboratory (SRNL). This work was produced by Battelle Savannah River Alliance, LLC, under Contract No. 89303321CEM000080 with the U.S. Department of Energy. The publisher acknowledges the U.S. Government license to provide public access under the DOE Public Access Plan (http://energy.gov/downloads/doe-publicaccess-plan).

Data Availability Statement: The data that support the findings of this study are available from the corresponding author upon reasonable request.

Conflicts of Interest: The authors declare no conflict of interest.

References

1. T.E. Schlesinger, J.E. Toney, H. Yoon, E.Y. Lee, B.A. Brunett, L. Franks, R.B. James, Cadmium zinc telluride and its use as a nuclear radiation detector material. Materials Science and Engineering R 32 (2001) 103-189.
2. G. Yang and R.B. James, Physics, in Physics, Defects, Hetero- and Nano-Structures, Crystal Growth, Surfaces and Applications: Part II, EDAX Elsevier (2009), p. 214-238.
3. S.D. Barthelmy, L.M. Barbier, J.R. Cummings, E.E. Fenimore, N. Gehrels, D. Hullinger, H.A. Krimm, C.B. Markwardt, D.M. Palmer, A. Parsons, G. Sato G, M. Suzuki, T. Takahashi, M. Tashiro, J. Tueller, The burst alert telescope (BAT) on the SWIFT midex mission. Space Science Reviews 120 (2005) 143-164.

4. S. Del Sordo, L. Abbene, E. Caroli, A.M. Mancini, A. Zappettini, P. Ubertini, Progress in the development of CdTe and CdZnTe semiconductor radiation detectors for astrophysical and medical applications. Sensors 9 (2009) 3491–3526.
5. P.M. Johns, J.C. Nino, Room temperature semiconductor detectors for nuclear security. J. Appl. Phys. 126 (2019) 040902.
6. M.D. Alam, S.S. Nasim, S. Hasan, Recent progress in CdZnTe based room temperature detectors for nuclear radiation monitoring. Prog. in Nuclear Energy 140 (2021) 103918.
7. M. Fiederle, D. Ebling, C. Eiche, D.M. Hofmann, M. Salk, W. Stadler, K.W. Benz, B.K. Meyer, J. Cryst. Growth 138 (1994) 529-533.
8. K. Kim, J. Hong, S. Kim, Electrical properties of semi-insulating $CdTe_{0:9}Se_{0:1}$: Cl crystal and its surface preparation. J. Cryst. Growth 310 (2008) 91–95.
9. U.N. Roy, A.E. Bolotnikov, G.S. Camarda, Y. Cui, A. Hossain, K. Lee, M. Marshal, G. Yang, R.B. James, Growth of $CdTe_xSe_{1-x}$ from a Te-rich solution for applications in radiation detection. J. Cryst. Growth 386 (2014) 43-46.
10. U.N. Roy, A.E. Bolotnikov, G.S. Camarda, Y. Cui, A. Hossain, K. Lee, G. Yang, R.B. James, Evaluation of $CdTe_xSe_{1-x}$ crystals grown from a Te-rich solution. J. Cryst. Growth 389 (2014) 99-102.
11. U.N. Roy, A.E. Bolotnikov, G.S. Camarda, Y. Cui, A. Hossain, K. Lee, W. Lee W, R. Tappero, G. Yang, R. Gul, R.B. James, High compositional homogeneity of $CdTe_xSe_{1-x}$ crystals grown by the Bridgman method. Appl. Phys. Lett. Mater. 3 (2015) 026102.
12. R. Gul, U.N. Roy, S.U. Egarievwe, A.E. Bolotnikov, G.S. Camarda, Y. Cui, A. Hossain, G. Yang, R.B. James, Point defects: Their influence on electron trapping, resistivity, and electron mobility-lifetime product in $CdTe_xSe_{1-x}$ detectors. J. Appl. Phys. 119 (2016) 025702.
13. R. Gul, U.N. Roy, A.E. Bolotnikov, G.S. Camarda, Y. Cui, A. Hossain, W. Lee, G. Yang, Y.Cui, A. Burger, R.B. James, Research Update: Point defects in $CdTe_xSe_{1-x}$ crystals grown from a Te-rich solution for applications in detecting radiation. Appl. Phys. Lett. Materials 3 (2015) 040702.
14. L. Hannachi, N. Bouarissa, Electronic structure and optical properties of $CdSe_xTe_{1-x}$ mixed crystals. Superlattices and Microstructures 44 (2008) 794-801.
15. A.E. Bolotnikov, G.S. Camarda, Y. Cui, G. Yang, A. Hossain, K. Kim, R.B. James, Characterization and evaluation of extended defects in CZT crystals for gamma-ray detectors. J. Cryst. Growth 379 (2013) 46-56.
16. S.A. Awadalla, J. Mackenzie, H. Chen, B. Redden, G. Bindley, M.C. Duff, A. Burger, M. Groza, V. Buliga, J.P. Bradley, Z.R. Dai, N. Teslich, D.R. Black, Characterization of detector-grade CdZnTe crystals grown by traveling heater method (THM). J. Cryst. Growth 312 (2010) 507-513.
17. U.N. Roy, S. Weiler, J. Stein, Y. Cui, M. Groza, V. Buliga, A. Burger, Zinc mapping in THM grown detector grade CZT. J. Cryst. Growth 347 (2012) 53-55.
18. N. Zhang, A. Yeckel, A. Burger, Y. Cui, K.G. Lynn, J.J. Derby, Anomalous segregation during electrodynamic gradient freeze growth of cadmium zinc telluride. J. Cryst. Growth 325 (2011) 10-19.
19. U.N. Roy, G.S. Camarda, Y. Cui, R. Gul, A. Hossain, G. Yang, J. Zazvorka, V. Dedic, J. Franc, R.B. James, Role of selenium addition to CdZnTe matrix for room-temperature radiation detector applications. Scientific Reports 9 (2019) 1620.
20. S. Hwang, H. Yu, A.E. Bolotnikov, R.B. James, K. Kim, Anomalous Te inclusion size and distribution in CdZnTeSe. IEEE Trans. on Nucl. Sc. 66 (2019) 2329-2332.

21. S.K. Chaudhuri, J.W. Kleppinger, O.M. Karadavut, R. Nag R, K.C. Mandal, Quaternary semiconductor $Cd_{1-x}Zn_xTe_{1-y}Se_y$ for high-resolution, room-temperature gamma-ray detection. Crystals 11 (2021) 827. https://doi.org/10.3390/cryst11070827
22. U.N. Roy, G.S. Camarda, Y. Cui, R. Gul, G. Yang, J. Zazvorka, V. Dedic, J. Franc, R.B. James, Evaluation of CdZnTeSe as a high-quality gamma-ray spectroscopic material with better compositional homogeneity and reduced defects. Scientific Reports 9 (2019) 7303.
23. L.M. Herraiz, A.F. Brana, J.L. Plaza, Vertical Gradient Freeze Growth of two inches $Cd_{1-x}Zn_xTe_{1-y}Se_y$ ingots with different Se content. J. Cryst. Growth 573 (2021) 126291. https://doi.org/10.1016/j.jcrysgro.2021.126291
24. J.W. Kleppinger, S.K. Chaudhuri, U.N. Roy, R.B. James, K.C. Mandal, Growth of $Cd_{0.9}Zn_{0.1}Te_{1-y}Se_y$ Single Crystals for Room-Temperature Gamma Ray Detection. IEEE Trans. on Nucl. Sc. 68 (2021) 2429-2434.
25. S.K. Chaudhuri, M. Sajjad, J.W. Kleppinger, K.C. Mandal, Correlation of Space Charge Limited Current and γ -Ray Response of $Cd_xZn_{1-x}Te_{1-y}Se_y$ Room-Temperature Radiation Detectors. IEEE Electron Device Lett. 41 (2020) 1336-1339.
26. S.U. Egarievwe, U.N. Roy, E.O. Agbalagba, B.A. Harrison, C.A. Goree, E.K. Savage, R.B. James, Optimizing CdZnTeSe Frisch-Grid Nuclear Detector for Gamma-Ray Spectroscopy. IEEE Access 8 (2020) 137530-137539.
27. R. Gul R, U.N. Roy, G.S. Camarda, A. Hossain, G. Yang G, P. Vanier, V. Lordi, R.B. James, A comparison of point defects in $Cd_{1-x}Zn_xTe_{1-y}Se_y$ crystals grown by Bridgman and traveling heater methods. J. Appl. Phys. 121 (2017) 125705.
28. A. Yakimov, D. Smith, J. Choi, S. Araujo, Growth and characterization of detector-grade CdZnTeSe by horizontal Bridgman technique. Proc. SPIE 11114 (2019), 111141N.
29. U.N. Roy, G.S. Camarda, Y. Cui, G. Yang, R.B. James, Impact of selenium addition to the cadmium-zinc-telluride matrix for producing high energy resolution X-and gamma-ray detectors. Scientific Reports 11 (2021) 10338.
30. J.H. Peterson, M. Fiederle, J.J. Derby, Analysis of the traveling heater method for the growth of cadmium telluride. J. Cryst. Growth 454 (2016) 45-58.
31. M. Funaki, T. Ozaki, K. Satoh, R. Ohno, Growth and characterization of CdTe single crystals for radiation detectors. Nucl. Instrum. Methods Phys. Res. A 436 (1999) 120-126.
32. Y. Wang, K. Kudo, Y. Inatomi, R. Ji, T. Motegi, Growth interface of CdZnTe grown from Te solution with THM technique under static magnetic field. J. Cryst. Growth 248 (2005) 406-411.
33. Y. Wang, K. Kudo, Y. Inatomi, R. Ji, T. Motegi, Growth and structure of CdZnTe crystal from Te solution with THM technique under static magnetic field. J. Cryst. Growth 275 (2005) e1551-e1556.
34. J.H. Peterson, Z. Cosenza, J.J. Derby, Stability-based optimization of ACRT for the growth of CZT by the traveling heater method. J. Cryst. Growth 579 (2022) 126446.
35. J.H. Peterson, J.J. Derby, The effects of ACRT on melt undercooling during the growth of CZT via the traveling heater method: Ekman versus Taylor-Gortler flows. J. Cryst. Growth 577 (2022) 126409.
36. A.L. Mokri, R. Triboulet, A. Lusson, A.T. Carli, G. Didier, Growth of large, high purity, low cost, uniform CdZnTe crystals by the "cold travelling heater metho. J. Cryst. Growth 138 (1994) 168-174.
37. B. Zhou, W. Jie, T. Wang, L. Yin, F. Yang, B. Zhang, S. Xi, J. Dong, Modification of growth interface of CdZnTe crystals in THM process by ACRT. J. Cryst. Growth 483 (2018) 281-284.

38. B. Hong B, S. Zhang, L. Zheng, H. Zhang, C. Wang, B. Zhao, Studies on thermal and interface optimization for CdZnTe crystals by unseeded Traveling Heater Method. J. Cryst. Growth 546 (2020) 125776.
39. U.N. Roy, S. Weiler, J. Stein, Growth and interface study of 2 in diameter CdZnTe by THM technique. J. Cryst. Growth 312 (2010) 2840-2845.